*30th EPS Conference on Contr. Fusion and Plasma Phys., St. Petersburg, 7-11 July 2003 ECA Vol. **27A**, O-3.3A*

Theoretical Understanding of Density Peaking: Dependence on Collisionality and on Heating Profiles

C. Angioni, A.G. Peeters, X. Garbet[1], F. Ryter, M. Apostoliceanu, A. Manini, G.V. Pereverzev, G. Tardini, ASDEX Upgrade Team

Max-Planck Institut für Plasmaphysik, IPP-EURATOM Association, Garching, Germany
[1] *Association Euratom-CEA sur la Fusion, CEA Cadarache, St Paul-Lez-Durance, France*

1. Introduction and theoretical standpoint

The shape of the density profile strongly affects the plasma performance. Density peaking is favourable for confinement, increases the bootstrap fraction as well as the fusion power in a burning plasma, while it has negative effects for magnetohydrodynamical stability and central impurity accumulation. The existence of an anomalous particle pinch leading to peaked density profiles, usually observed in tokamaks even when the fuelling is only peripheral, has been recently assessed in dedicated experiments in L–mode plasmas with zero loop voltage [1, 2]. Such an anomalous particle pinch usually exceeds the neoclassical Ware pinch. However in high density plasmas in H–mode, both the steady state and the time evolution of the density profiles were found to be consistent with a Ware pinch alone in AUG [3] and in JET [4].

Previous theoretical works have proposed two mechanisms leading to the presence of out–of–diagonal terms in the anomalous particle flux. One is based on turbulent thermodiffusion [5], and predicts a particle flux proportional to the logarithmic gradient of the temperature. A thermodiffusive contribution to the particle flux is found as well in quasi–linear estimates derived from a drift wave ITG and TEM fluid transport model [6]. The second mechanism is usually called "Turbulent Equi–Partition" (TEP) [7] , and predicts a pinch velocity proportional to the curvature of the magnetic field.

Following more recent theoretical developments [8], here we propose first a minimal 1D linearised collisionless drift wave model, describing ITG and TEMs, which leads to a quasi–linear expression of the particle flux including contributions from both the above mentioned mechanisms,

$$\begin{cases} -\left(\omega - \tilde{\omega}_{De}\right)\hat{n}_e + \tilde{\omega}_{De}\hat{T}_e - \left(\tilde{\omega}_{De} - \omega_{*e}\right)\hat{\phi} = 0 \\ -\left(\omega - \mathrm{X}\,\tilde{\omega}_{De}\right)\hat{T}_e + \frac{2}{3}\omega\,\hat{n}_e + \omega_{*e}\left(\eta_e - \frac{2}{3}\right)\hat{\phi} = 0 \\ \text{ion equations: continuity, energy balance, (parallel motion)} \\ \text{quasi-neutrality } (\Rightarrow \text{ambipolarity}) \text{ (adiabatic free electrons)} \end{cases} \tag{1}$$

The first two equations describe continuity and energy balance for the trapped electrons. Here ω is the complex mode frequency, $\tilde{\omega}_{De}$ is a general curvature drift frequency, specified later, and ω_{*e} is the diamagnetic frequency. Electron density and temperature perturbations are normalized in the form $\hat{n}_e = \delta n_e/n_e$, while the electrostatic potential is normalized as $\hat{\phi} = e\delta\phi/T_e$. The two equations for the trapped electrons are coupled with a set of equations describing the ion response, which do not need to be specified in our derivation. Ions can be described by gyrofluid equations, like in the GLF23 transport model [9], or by a set of drift–fluid equations, like in the Weiland model [6]. Our conclusions will not be specific to any choice of the equations describing the ion dynamics. In the present generic model, specific choices of the adiabatic compression index X and of the drift frequency $\tilde{\omega}_{De}$ allow this model to describe the same equations of transport models already proposed in the literature and used in transport modelling. In particular taking $X = 5/3$ and $\tilde{\omega}_{De} = \omega_{De0}$, where $\omega_{De0} \doteq 2\,c_s\,(k_\perp \rho_s)/R$, the previous model describes the same electron equations as the Weiland model, in the electrostatic collisionless form presented in [6] ($c_s = \sqrt{T_e/m_i}$, $\rho_s = c_s/\Omega_{ci}$, $\Omega_{ci} = Z_i eB/m_i$). The choice $X = 5/3$ and $\tilde{\omega}_{De} = \lambda_T \omega_{De0}$, where $\lambda_T = 1/4 + 2/3s$, provides a 1D linearised version of a 3D non–linear model recently proposed in [8]. Finally, choosing $X = 4/3\,(0.7 - i0.8)$ and $\tilde{\omega}_{De} = f_s(s, q, \alpha)\omega_{De0}$, where $f_s(s, q, \alpha)$ is a function of magnetic shear s, safety factor q and Shafranov shift parameter $\alpha = -q^2 R d\beta/dr$ matching the results of a 3D gyrokinetic code [9], the model in Eq. (1) describes the same equations of the GLF23 model in the electrostatic collisionless limit [9]. The quasi–linear estimate of the particle flux $\langle \delta n_e\ \delta v_{Ex} \rangle$ can be computed analitically for such a model, adopting analogous procedure of [6], and reads,

$$\frac{\Gamma_{ql}}{n_e} = -\,f_t\ D_{ql}(\gamma, \omega, k_\theta, ...)\ \left[\ \frac{\partial_\rho n_e}{n_e}\ +\ C_T\ \frac{\partial_\rho T_e}{T_e}\ +\ 2\,\frac{\tilde{\omega}_{De}}{\omega_{De0}}\left(1\ +\ \frac{2}{3}C_T\right)\frac{|\partial_\rho B|}{B}\ \right]. \tag{2}$$

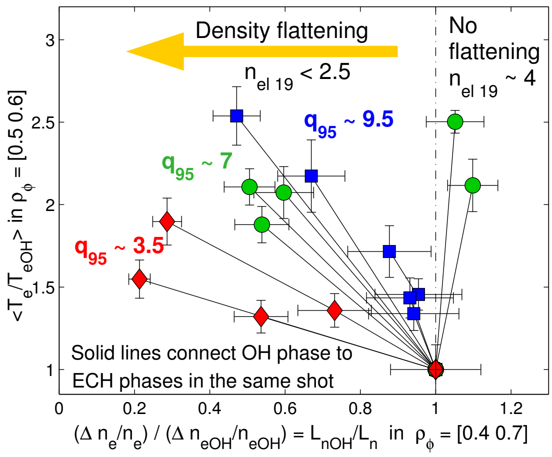

Fig. 1. *Density peaking ratio ECH to OH phase w.r.t.* T_e/T_{eOH}*, for different values of* q_{95}*.*

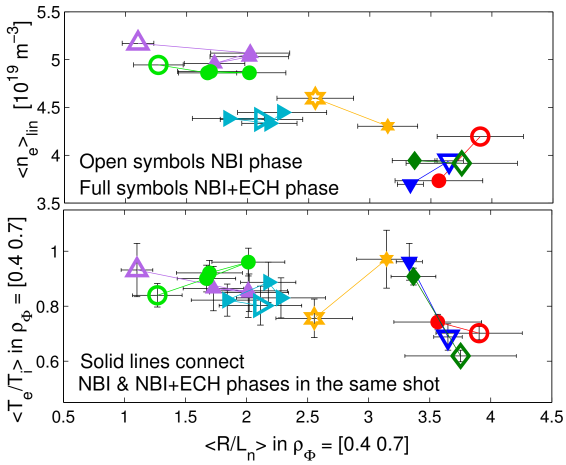

Fig. 2. *Density peaking* (R/L_n) *in NBI and NBI+ECH phases w.r.t density (a), and* T_e/T_i *(b).*

Here D_{ql} is the quasi–linear diffusion coefficient, while C_T is the thermodiffusion factor. Dependences on electron plasma parameters are made explicit by the procedure adopted to handle the fluid equations, while dependences on ion plasma parameters are hidden in the complicated dependences of D_{ql} and C_T on the mode frequency ω and growth rate γ. These in particular adjust in order to satisfy the quasi–neutrality condition, being eigenvalues of the dispersion relation, and ensure the ambipolarity of the particle fluxes. While we shall not provide here the full expression of D_{ql}, rather we just underline that it is positive for any value of ω and γ, we focus on the coefficient C_T ($\hat{\omega}_r = \omega_r/\omega_{De0}$, $\hat{\gamma} = \gamma/\omega_{De0}$),

$$C_T = \frac{2\,\hat{\omega}_r \;-\; (X_r + 5/3)\; f_s(s,q,\alpha) \;+\; X_i\;(\hat{\omega}_r - f_s^2)\,/\hat{\gamma}}{\hat{\omega}_r^2 + \hat{\gamma}^2 - \hat{\omega}_r\,(4/3 + 2X_r)\,f_s + [10/9 + X_r\,(X_r + 4/3)]\,f_s^2 + X_i f_s\,(X_i f_s - 2\hat{\gamma} - 2 f_s^2/3\hat{\gamma})}. \quad (3)$$

This term changes sign depending on the value of the real frequency of the mode. The threshold between a positive and a negative value depends on the adiabatic compression index, and thereby is directly related to the fluid closure assumptions. For usual monotonic electron temperature profiles, the thermodiffusive flux is directed inwards when the mode rotates in the ion drift direction (ITG), while it can be directed outwards when the mode rotates in the electron drift direction (TEM). The last term in Eq. (2) is the curvature pinch. In the limits $|\hat{\omega}| >> 1$, or $\hat{\gamma} >> 1$, $C_T << 1$ and the curvature term becomes $2/R\,(\tilde{\omega}_{De}/\omega_{De0})$. The latter, assuming the model proposed in [8], can be written in the form $2\lambda_t/R$, which gives, from Eq. (2), "natural density profiles" $n(r)/n(r=0) = exp(-\int_0^r (2\lambda_t/R)dr)$, the form predicted by TEP models. This shows that TEP prescriptions can be included in a 1D, fluid drift wave transport model suited for transport simulations.

Finally, Eq. (3) for C_T shows that the magnitude of the thermodiffusion factor strongly depends on $\hat{\omega}_r$ and $\hat{\gamma}$, as well as on the closure in a fluid model. Strong effects of the electron temperature profile on the density profile must be expected only in specific operational regimes which imply plasma parameters, and related frequencies of the dominant instabilities, in the domain maximising C_T. This consideration motivates a characterisation of the experimental behaviour of the density profiles in the presence of additional heating: the analysis is performed on experimental results collected in the AUG tokamak.

2. Experimental observations and comparison with theory predictions

At low density ($2\ 10^{19}\ \mathrm{m}^{-3}$), in AUG central ECH produces a flattening of the density profile [10]. This is observed in both sawtoothing and non–sawtoothing ($q_0 > 1$) discharges. Central ECH mainly modifies the electron temperature profile while keeping constant R/L_{Te} [11]: the variation of R/L_n must be rather related to a variation of T_e (Fig. 1). At a fixed value of q_{95}, an increase of T_e produces a decrease of $\nabla n_e/n_e$. For the same increase of T_e, the decrease of $\nabla n_e/n_e$ becomes smaller at higher values of q_{95}. The small coupling between electrons and ions in these plasmas leads to ratios T_e/T_i ranging from 1.5 in OH up to larger than 2 with ECH (L_{Ti}/L_{Te} larger than 1.5) in the confinement region (T_e from Thomson scattering and ECE diagnostics, T_i from NPA). In case of plasmas with higher density ($4\ 10^{19}\ \mathrm{m}^{-3}$), the central flattening is not observed any more (Fig. 1). In this case the stronger coupling between electrons and ions leads to a smaller T_e/T_i ratio both in OH ($T_e/T_i \simeq 1.2$) and ECH ($T_e/T_i < 2$).

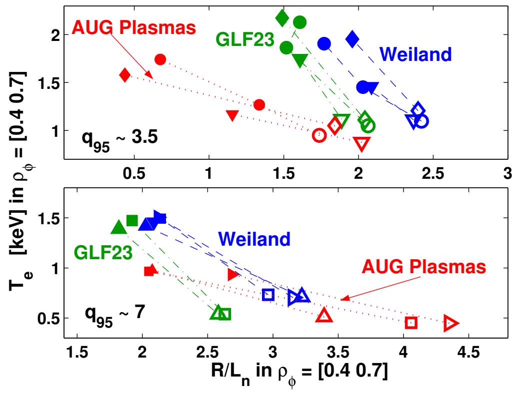

Fig. 3. (↑) *Transport simulations (GLF23 green and Weiland blue) of OH (open symbols) and ECH (full symbols) phases in low density shots. Predicted R/L_n decreases with ECH, but less than in exps.*
Fig. 4. (→) *Simulations (GLF23) of high density plasmas with 5 MW NBI (▽), 2.5 MW NBI and 2.5 MW centr. electron (◁), and 2.5 MW central ion (△), and 2.5 MW centr. 50% ion and 50% electron heating (▷), without (a) and with (b,c) Ware pinch.*

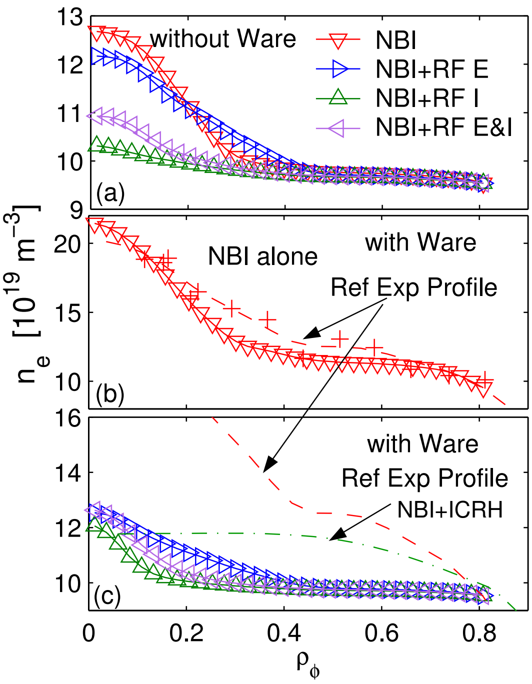

The disappearance of the density flattening due to central ECH in plasmas at higher density motivates the investigation of the density response to central electron heating in regimes in which the ratio T_e/T_i is around or smaller than 1. These experiments are performed at low to intermediate densities, with dominant ion heating provided by NBI, on top of which central ECH has been applied (H–mode plasmas) [12]. In the regime of plasma parameters prevailing in these experiments gyrokinetic calculations, as well as transport fluid models (GLF23, Weiland), indicate that the dominant instability is an ITG. The electron heat flux in the confinement region, from the NBI to the NBI+ECH phase, increases by a factor even larger than 2. Although such a variation is not as large as the one obtained starting from OH conditions, we underline that a model linking the density flattening to the variation of the electron heat flux (by assuming a particle diffusivity proportional to the anomalous power balance heat diffusivity) [10] would imply a significant flattening of the density profile in these conditions. On the contrary, it is observed that the measured variations of the density peaking remain practically within the errorbars: only at the lowest densities (and largest R/L_n) a small flattening is observed, while at larger densities the density profile remains unchanged or even steepens slightly (Fig. 2). GLF23 provides good (lowest density plasmas) to excellent (higher density plasmas) simulations (T_e, T_i, n_e) in these conditions (ASTRA transport code).

In conclusion, in AUG clear density flattening with central ECH is observed only at low densities, with large T_e/T_i (and L_{Ti}/L_{Te}) ratios. In this domain of plasma parameters linear gyrokinetic calculations show that the dominant instability is a TEM. In these conditions the observed density flattening is therefore consistent with an outward particle flux driven by the electron temperature gradient, as obtained in Eq. (2). Transport simulations of plasmas in these conditions show that a density flattening is indeed predicted by drift wave transport models like Weiland or GLF23. However the predicted flattening is usually smaller than the experimental one (Fig. 3). Moreover for GLF23, it has been necessary to ensure that the dominant instability was a TEM, by imposing sufficiently small ion temperature gradients: the GLF23 model most often finds the most unstable mode rotating in the ion drift direction in these conditions, while in the same conditions the gyrokinetic code GS2 finds a most unstable mode rotating in the opposite direction. The critical role of T_e/T_i is found as well in recent turbulent fluid simulations of particle transport, describing collisionless ITG and TEMs [8]: a hollow density profile is obtained when the ratio T_e/T_i is above 3.

Further experimental observations of density flattening with central heating have been collected in high density plasmas with central ICRH, and T_e/T_i ratios very close to 1 [10]. The ICRH power absorbed by the electrons in these conditions is smaller than 30% (calculations with the TORIC code). This suggests that density flattening in these conditions is rather due to the more centrally localised ion heating provided by ICRH, as compared with NBI. This is consistent with the predictions of fluid drift wave transport models, as illustrated in Fig. 4a by the results of transport simulations with the GLF23 model and excluding the Ware pinch. Here the same set–up of the experiments described in [10] has been adopted in the simulations, and both a phase of full NBI heating (5 MW) and a phase with half of the NBI power replaced by more centrally localised RF heating are simulated. Different ratios of $P_{RF\,i}/P_{RF\,e}$ are considered. Both the simulations in which 50% or 100% of the RF power is absorbed by the ions imply a very strong flattening of the density profile. This is explained by the increase of the global plasma diffusivity, proportional to the mode growth rate, while the particle flux is kept unchanged. Roughly, in these conditions the GLF23 model behaves similarly to the model $D \propto \chi_{PB}^{turb}$ [10]. We mention that in these conditions the Ware pinch plays a non–negligible role, as established experimentally [3] and explained theoretically [13]. This is illustrated as well in Fig. 4b, in which the NBI phase is simulated including the Ware pinch, and compared to a reference representative experimental profile. Simulations in the case of central RF heating and including the Ware pinch are in Fig. 4c. The predicted density profiles are too flat w.r.t. the experimental one. Such a flattening is numerically enhanced by the artificial procedure of defining an effective diffusion coefficient in GLF23, which becomes questionable in the presence of very small density gradients or almost zero particle fluxes.

3. Dependence on collisionality and conclusions

Density peaking has been observed to drop with increasing collisionality, in AUG H–mode plasmas with NBI heating [13]. The same dependence is observed in plasmas with ICRH+NBI heating (Fig. 5). This behaviour has been explained by the effect of collisions on drift wave (ITG+TEMs) instabilities: anomalous inward particle flux contributions are found to drop more quickly towards high collisionality, as compared with the drop of the outward contributions. The anomalous particle fluxes are dominant at low collisionality, Ware pinch effects become important only at high collisionality [13] (details on transport modelling in [14]).

In conclusion, a simple fluid model describing ITG and TEMs prescribes the existence of an electron thermodiffusive particle flux whose magnitude and sign depend critically on the real frequency and growth rate of the dominant instability. Electron thermodiffusion is directed outward for TEMs, inward for ITG modes. A set of experimental evidences consistent with this theoretical picture has been collected in AUG. In particular clear density flattening with central ECH is observed at low density (dominant TEM), while this effect is reduced and disappears when central ECH is applied to NBI heated plasmas (dominant ITG). The ratio T_e/T_i is likely to play a pivotal role (large R/L_n and/or small R/L_{Ti} can drive the mode unstable in the TEM domain as well). At very high density central ICRH (dominant ion heating) also flattens the density profile (dominant ITG). GLF23 provides in general good transport simulations of the density profiles when ITGs are the dominant instability, while both GLF23 and Weiland predict a too small flattening in the case of central ECH heating in low density plasmas. The theoretical and experimental results presented here indicate that density flattening with central electron heating occurs only when TEM is the dominant instability. This conclusion needs certainly further experimental confirmation. It would have important implications for ITER.

One of the authors (CA) acknowledges financial support for this work from the EURATOM programme of the European Community in the form of a Marie Curie Individual Fellowship.

References

[1] Hoang G T *et al* 2003 *PRL* **90** 155002.
[2] Zabolotsky A *et al* 2003 *PPCF* **45** 735.
[3] Stober J *et al* 2001 *NF* **41** 1535.
[4] Valovic M *et al* 2002 *PPCF* **44** 1911.
[5] Coppi B, Spight C 1978 *PRL* **41** 551.
[6] Weiland J *et al* 1989 *NF* **29** 1810.
[7] Baker DR and Rosenbluth MN 1998 *PoP* **5** 2936, and Refs [3-8] therein.
[8] Garbet X *et al* 2003 *PRL* to be published.
[9] Waltz R E *et al* 1997 *PoP* **4** 2482.
[10] Stober J *et al* 2003 *NF* to be published.
[11] Ryter F *et al* 2001 *PRL* **86** 5498.
[12] Manini A *et al* 2003 this conference.
[13] Angioni C *et al* 2003 *PRL* **90** 205003.
[14] Angioni C *et al* 2003 *PoP* to be published.

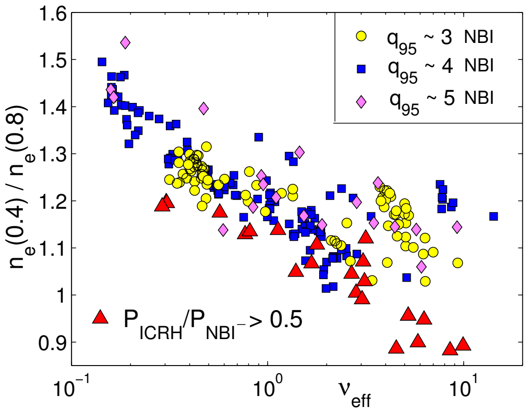

Fig. 5. Density peaking vs $\nu_{\rm eff} = \nu_{ei}/\omega_{De0}$.